ISBN: 978-3-95450-262-2 ISSN: 2673-5350 doi: 10.18429/JACoW-IBIC2025-TUDI01

A REVIEW OF SPACE CHARGE COMPENSATION DIAGNOSTICS

E. L. Flannigan*, O. Tarvainen, R. Abel, D. Faircloth, A. Garcia Sosa, D. Morris
STFC ISIS Neutron and Muon Source, Harwell, UK
D. R. Emerson, B. John, K. Jonathan, STFC Scientific Computing Department, Warrington, UK

Abstract

The space charge of high-intensity ion beams makes it challenging to transport the beam through the Low Energy Beam Transport (LEBT) and inject it into the subsequent accelerator. Space charge compensation (SCC) is a process that lowers the space charge of an ion beam by trapping either positive ions or electrons, created by interaction of the beam with residual gas. The compensating secondary particles reduce the beam potential and the space charge-induced divergence of the beam. Significant beam losses during SCC build-up necessitate minimising the SCC time of pulsed high-current ion beams. To address this, diagnostic techniques are used to measure the SCC degree or time or optimise the background gas pressure. These techniques include emittance meters, beam profile monitors, wire scanners, retarding field analysers, Langmuir probes and optical sensors. Such diagnostics are applicable to positive and negative ion beams, with unique challenges based on the specific ion beam and residual gas used. We review common SCC diagnostic techniques to measure various beam characteristics. The diagnostic techniques are often invasive, stopping the beam, changing its characteristics and affecting the local SCC degree. It is therefore important to develop non-invasive diagnostic techniques and to complement diagnostic measurements with particle-in-cell simulations.

INTRODUCTION

Space charge forces in high-intensity ion beams defocus the beam, leading to beam losses and emittance growth. Space charge compensation (SCC) reduces or eliminates these effects. SCC occurs when an ion beam propagating through a residual or injected gas ionises it through the reaction:

$$A^q + B \rightarrow A^q + B^+ + e^-,$$

where A is the ion beam species, q is the ion beam charge state and B is the gas species. The secondary particles produced by this ionisation reaction (electrons and positive ions) are either repelled or trapped by the beam potential depending on their polarity. The trapped particles reduce the beam potential to a steady state determined by the ionisation rate of the background gas and loss of compensating (and uncompensating) particles. The SCC degree, η(r,z), is given by [1]:

$$\eta = 1 - \frac{\phi_c(r,z)}{\phi_u(r,z)}, \quad (1)$$

where ϕ_c(r,z) is the beam potential of the compensated beam and ϕ_u(r,z) is the potential of the uncompensated beam. Due to the increased mobility of electrons, the steady-state compensation degree of positive ion beams can be limited. However, in addition to electrons created from ionisation of the residual gas, secondary electrons are created when the beam hits surfaces within the beamline and provide an additional source of compensating particles. In contrast, at some gas pressures and with certain beam parameters, negative ion beams can undergo overcompensation due to the heavier positive compensating particles.

The time it takes to build up to this steady-state compensation degree, or SCC time, can be estimated by:

$$\tau = \frac{\eta}{n_g \sigma(E_b) v_b}, \quad (2)$$

where n_g is the gas number density and v_b is the speed of the beam. The ionisation cross section of the reaction, $\sigma(E_b)$, depends on ion beam species, species of the background gas and the energy of the beam. For an H^+ beam the compensating reaction $H^+ + H_2 \rightarrow H^+ + H_2^+ + e^-$ has an ionisation cross section of 2.11 x 10^{-20} m^2 [2]. At a background gas pressure of 1 x 10^{-5} mbar and an often-assumed SCC degree of 0.9, the SCC time for a 65 keV H^+ is 50 µs. This estimation assumes that all compensating particles are trapped by the beam potential and its validity is dependent on the loss rate of the compensating particles. When the beam potential is the only trapping potential, Eq. (2) is a better approximation for negative beams, where the mobility of the compensating particles is lower.

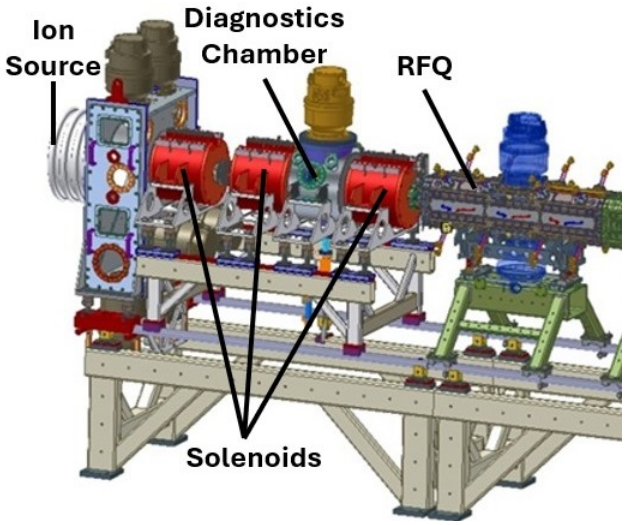

Figure 1: A schematic of the magnetostatic LEBT of the Front-End Test Stand at ISIS Muon and Neutron Source. It consists of three solenoids for focusing into the RFQ.

For a continuous beam, compensation is reached after the transient build-up time. Once a steady state is reached, the

* erin.flannigan@stfc.ac.uk

ISBN: 978-3-95450-262-2 ISSN: 2673-5350 doi: 10.18429/JACoW-IBIC2025-TUDI01

compensation will remain stable. In contrast, a pulsed beam will experience this build-up time with each new pulse. In this case, the steady-state compensation degree is dependent on the pulse duration relative to the SCC time. If the pulse duration is significantly longer than the SCC time it will behave similarly to a continuous beam but undergo the SCC process at the start of each new pulse. When the pulse duration is similar to but greater than the SCC time the beam will be undercompensated at the beginning of the pulse but compensated after the SCC time, causing variations in the beam transport. Finally, when a beam has a pulse duration shorter than the SCC time it will remain essentially uncompensated.

For short beam pulses, the SCC time may cause significant power consumption as the radio frequency quadrupole (RFQ) and linac must produce pulses longer than the beam pulse, regardless of the useful fraction, or a chopper must be used in the Medium Energy Beam Transport (MEBT) to chop the unwanted fraction of the beam after the RFQ. The addition of a chopper in the LEBT would remove any SCC. Reducing the SCC time is therefore of particular importance for pulsed ion beams. Reduction in SCC time is dependent on the gas pressure, as all other variables in Eq. (2) are a function of the beam energy, which is fixed by the design of the system. Decreasing the SCC time requires higher background gas pressures that may lead to an increase in beam stripping losses.

SCC occurs in the Low Energy Beam Transport (LEBT), where the ion beam is transported and matched into the subsequent accelerating structure, typically an RFQ. Both electrostatic and magnetostatic LEBTs are used for this focusing. In an electrostatic LEBT, the electric field from the focusing elements either attract or repel the secondary particles. These secondary particles therefore are not accumulated by the beam potential and no SCC can occur. The beam intensity is limited in an electrostatic LEBT, due to the large divergence and size of high intensity beams when uncompensated. However, electrostatic lenses at the entrance and exit of the beamline can also be used to trap secondary particles, aiding the SCC process.

High-current accelerator applications typically use magnetostatic LEBTs with magnetic focusing solenoids (e.g. ISIS, CERN, J-PARC). Figure 1 shows an example three-solenoid LEBT of the Front-End Test Stand at the ISIS Muon and Neutron Source, designed to transport a pulsed 60 mA, 65 keV H^- beam and match it to the subsequent 3 MeV RFQ [3]. The residual gas from the ion source can provide the beamline pressures necessary to facilitate SCC. Significant beam losses occur during the SCC build-up time as the solenoid settings are selected to focus the beam once it has reached a steady state.

This beam loss can lead to erosion and activation of the preceding accelerating structure. It is therefore crucial to understand the SCC process and minimise the SCC time, without inducing additional beam losses. Multiple diagnostic techniques used to study the SCC process are detailed in the following section, with a focus on their application to hydrogen ion beams. Heavier ion beams typically have lower current and therefore do not experience the same space charge issues, with the exception of electromagnetic isotope separators that can produce tens of mA of positive heavy element beams.

DIAGNOSTICS

Diagnostic techniques used to measure the SCC of an ion beam are generally used to measure a specific beam characteristic or compensation dynamic as the beam undergoes SCC. Commonly measured characteristics are the beam intensity, spatial distribution, emittance or potential. Multiple diagnostic techniques are often used in combination to provide a more complete representation of the SCC process. Further details on many diagnostic techniques in the LEBT (e.g. Faraday cups, beam current transformers, scintillation viewers, wire scanners, wire grids, Allison scanners, pepper-pots) can be found in [4].

Intensity

The total beam current can be used to measure SCC time only via several measurements quantifying transmission losses. Faraday cups and beam current transformers (BCTs) are two commonly used diagnostic devices for beam current measurements. While Faraday cups are a commonly used diagnostic for current measurements [4], they do not provide useful measurement of SCC and can perturb the compensation process.

BCTs are commonly used as a non-invasive, time-resolved monitor of pulsed beam currents, although specialised DC current transformers that use magnetic saturation are also in use [5]. A BCT consists of a toroidal magnetic core through which the ion beam passes and acts as a one-turn primary winding. A coil wound on the core acts as the secondary winding. The current can then be calculated from the output signal of this coil. Two BCTS, one at both the entrance and exit of an acceptance-limited component (e.g. an RFQ), are required to use the time-resolved beam current as a SCC diagnostic.

Figure 2 shows an H^- beam current measured by BCTs in the LEBT and at the exit of the RFQ of the ISIS Muon and Neutron Source. During measurement, the LEBT solenoid fields are optimised for beam transport of the steady-state part of the pulse. A period of low H^- beam transmission through the RFQ may be seen in the first ~50 µs of the pulse. This low transmission is more clearly illustrated in the normalised difference between the two beam pulses. This difference is determined by normalising the pulse in both the LEBT and the RFQ to the average current of their respective steady states (from t=100-165 µs). The difference between the two resulting pulses is then taken. During the beginning of the pulse when there is a large beam mismatch, significant current is lost at the entrance of the RFQ. As compensation occurs, the beam is transported through the RFQ. Measurement of this current difference can therefore provide the SCC time.

ISBN: 978-3-95450-262-2 ISSN: 2673-5350 doi: 10.18429/JACoW-IBIC2025-TUDI01

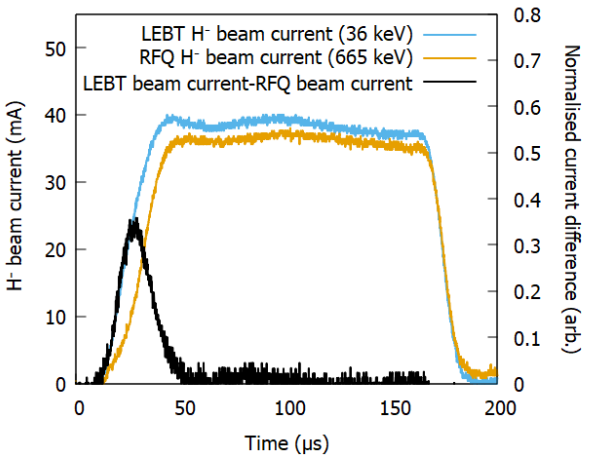

Figure 2: The current of a pulsed H^- beam in the ISIS Muon and Neutron Source LEBT (36 keV) and at the exit of the RFQ (665 keV). The normalised difference between the LEBT and RFQ H^- beam current shows a period of low transmission in the first ~50 μs.

Spatial Distribution

The beam profile, or spatial distribution of beam particles, cannot measure SCC degree but is often used to quantify optimum gas pressure for SCC versus the beam losses induced by that gas. Without SCC, the ions will repel each other, broadening the transverse profile of the beam. This beam distribution is improved when the beam is compensated. Many methods, both invasive and non-invasive, are used to measure the spatial distribution of the beam. Wire scanners, wire grids or 'harps' and scintillation viewers are three common, invasive diagnostic techniques for measuring the transverse beam profile.

Wire scanners consist of a thin wire that is moved transversely through the beam. The signal measured by the wire corresponds to the local charge density at that wire position, providing a signal vs wire position or beam profile. If a wire scanner is also used in an orthogonal direction, a 2D beam distribution can be found. Bykov *et al.* [6] used a modified wire scanner to measure the beam profile of a continuous 22 keV H^- beam under various residual gas pressures. An ideal residual gas pressure can then be found that optimises the current, cross-sectional area and current density by finding a balance between ideal conditions for SCC without inducing further ion stripping losses. Similar results were found by Peng *et al.* [7] when measuring the beam profile of 35 keV, 90 mA H^+ and 40 keV, 10 mA He^+ continuous beams with various gas types and gas pressures.

Wire grids, or harps, consist of a frame with many thin wires stretched across of it, typically oriented both horizontally and vertically. As the ion beam passes through the grid the current from each wire is measured. The current vs the position of the grids provides a beam profile. Unlike wire scanners, the beam intensity over the entire profile is sampled simultaneously. A study by von Jagwitz-Biegnitz *et al.* [8] used a wire grid to measure the shape of a 10 keV H^- beam profile versus time. The beam profile formed evolves as it compensates.

An invasive but direct method of measuring the beam profile is using a charge-coupled device (CCD) camera to observe the light emitted by a scintillation screen as it is hit by the beam. Beauvais *et al.* [9] used a scintillation screen to measure the transverse beam profile of a pulsed, 500 keV H^+ beam at currents from 0.5 to 15 mA to determine the relationship between residual gas pressure and beam current on the beam spot size. Toivanen *et al.* [10] used scintillation screens to study the effect of beamline gas pressure on the beam emittance due to SCC for a continuous 40-150 μA Ar ion beam with charge states 6+, 8+, 9+ and 11+. The effect of adjusting the extraction voltage and gas species (N_2, Ar, He) was also studied.

Misra *et al.* [11] developed a non-invasive technique using a CCD camera to measure the fluorescence of residual H_2 gas or injected Ne gas as a 5 mA, 75 keV H^+ beam undergoes compensation. A reduction of ~34 % in the rms beam size was found from the additional compensation provided by the addition of Ne gas to the existing residual gas.

Emittance

The emittance of an ion beam is a measure of the area or volume of the beam in position-momentum space, providing a quantity to characterise the beam quality. As in the measurement of beam spatial distribution, the beam emittance cannot provide a direct measurement of SCC degree. However, an uncompensated beam will experience emittance growth, i.e. a compensated beam will have smaller emittance at the end of the LEBT [12]. This can be useful when determining the optimum gas pressure of the system.

To measure the emittance in low-energy ion beams, slit-slit, slit-grid, Allison scanners and pepper-pots are the most common diagnostic devices. A slit-slit emittance meter provides a 2D transverse (i.e. x and x' or y and y') measurement of the emittance. It consists of two parallel slits in front of a collector (e.g. a Faraday cup). The first slit selects a narrow position and the second slit selects an angular slice of the resulting beamlet. By scanning both slits, a full 2D distribution can be determined. To measure this in 4D, two independent 2D scans may be run or two sets of 4-jaw slits may be used. Slit-based emittance measurements suffer from issues of slit deformation, secondary electron emission and tolerances.

A slit-grid emittance meter consists of a narrow slit in front of a grid of collectors. These collectors, often called 'harps', are used to measure the beam profile. The entrance slit is scanned across, giving the beam position, while the angular distribution is determined by the location of the collectors measuring that beamlet. It is less mechanically complex than the slit-slit meter but still requires multiple scans. Slit-grid meters have been repeatedly used to compare measured emittance to simulated emittance with respect to the SCC process and the effects of injecting gas of various types at various pressures [13–15].

Allison scanners [16] consists of both an entrance and exit slit. Between these two slits, an electrostatic deflector

ISBN: 978-3-95450-262-2 ISSN: 2673-5350 doi: 10.18429/JACoW-IBIC2025-TUDI01

can be voltage swept such that the beamlet is deflected based on its initial divergence. A collector (e.g. a Faraday cup) is used to measure the transmitted particles. The entrance slit is scanned to determine the position. The voltage sweep improves the resolution and decreases the measurement time compared to the slit-slit meter. Allison scanners are more applicable to the measurement of the fast SCC process, as only one mechanical scan is required [17]. This requires recording time-resolved currents at each position-plate voltage setting and post-analysis.

A pepper-pot emittance meter removes the scanning requirements of other emittance meters, providing a single-shot measurement of emittance. The pepper-pot consists of a plate with an array of small holes, placed in front of a viewing screen. The location of the holes provides the position of the beam, while the displacement of the beamlets on the view screen provide the divergence angles. Gobin *et al.* [18] used a pepper-pot to measure the emittance of a continuous 95 keV, 92 mA H^+ beam with ^{84}Kr or Ar gas injected into the beamline to improve the SCC. They found the injected gas reduced the beam emittance by a factor of 3 with minimal stripping losses induced. While this does not provide a measurement of the SCC time and degree, it can be used to optimise the gas type and pressure.

Potential

Time-resolved measurement of the beam potential is the only method that can determine the SCC degree, by comparison of the potential before and after compensation. It can also be used to measure the SCC time. The beam potential may be determined by measuring the energy of the secondary particles either repelled by or captured by the beam. As the starting energy of these secondary particles is negligible, their kinetic energy will be given by the potential at their origin point. The measured energy will therefore provide the beam potential. Langmuir probes, energy-dispersive spectrometers and retarding field analysers (RFAs) are used to measure the beam potential or energy of the secondary particles.

Langmuir probes work by inserting an electrode into a plasma to measure the electron temperature, electron density and electric potential. The bias voltage of the probe is swept while measuring the plasma current changes. Jakob *et al.* [19] used a decompensation electrode to adjust the compensation degree of the ion beam and measure the resulting beam potential with a Langmuir probe. Holmes [20] used a Langmuir probe to measure that the beam potential of a 20 keV, 10 mA He^+ continuous beam decreased with increased gas pressure and with decreased beam energy. However, it is noted in both studies that insertion of the probe will influence the ion beam and could therefore affect the SCC process.

Kreisler *et al.* [21] and Reidelbach *et al.* [22] used energy-dispersive spectrometers to investigate the time-resolved beam potential, and therefore the SCC time and degree, of a 0.01-1.6 mA, 15-45 keV Ar^+ beam and a 3.1 mA, 10.7 keV He^+ beam, respectively. In both studies, the secondary particles radially repelled by the beam potential were separated by their energy using an electrostatic analyser and then measured with a position sensitive detector. The energy distribution of the secondary particles was measured at multiple gas pressures to determine the SCC degree.

RFAs, four-grid analysers or three-grid energy analysers may be used for non-invasive measurement of the secondary particle energy. An example of an RFA, which uses a three-grid design is presented in Fig. 3. This shows the working principle for a positive ion beam with positive secondary ions collected by the RFA. Each design includes a collection plate with a series of three or four grids preceding it. The grid closest to the collection plate can be biased to repel secondary electrons produced on the collection plate. The next grid from the collection plate provides the particle energy discrimination; an adjustable retarding voltage is swept while measuring the signal on the collection plate. In the case of a four-grid analyser, a potential can be placed on the next grid to suppress electrons coming from the beamline. Both designs have a grounded first grid. The maximum energy of the secondary particles varies based on the system but are often on the order of tens or hundreds of eV; simulations indicate that for a 65 keV, 30 mA H^- beam, the maximum energy of the electrons is 182 eV [23]; for a 500-1000 µA O^{6+} beam with an extraction voltage of 15 kV there is a predicted maximum secondary particle energy of 4-10 eV [24].

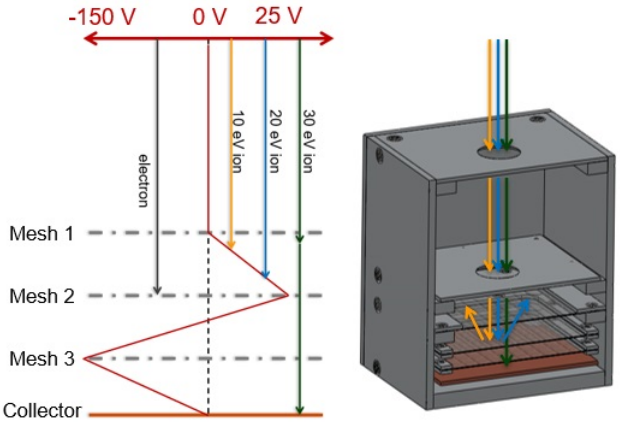

Figure 3: A 3D CAD model of an RFA and the working principle for measurement of positive secondary ions. The central grid is biased to 25 V, so positive ions with an energy less than 25 eV will be reflected by the retarding field. This figure is modified from D. Winklehner *et al.* [25].

While multiple design variations are used, the measurement mechanism remains the same. These various designs have been used as a SCC diagnostic to determine the time-resolved beam potential for H^+, H^-, He^+, Ar^+ and O^{6+} beams [24–28].

Optical Emission

Collisions of the ion beam or the secondary particles with the residual gas will excite the gas particles, producing photons. These light emissions may then be measured to provide information on the ion beam or on the SCC process.

ISBN: 978-3-95450-262-2 ISSN: 2673-5350 doi: 10.18429/JACoW-IBIC2025-TUDI01

In addition to measuring the beam profile using beam-induced and electron-induced light emission [11], diagnostics are being developed for the time-resolved measurement of light intensity emitted by pulsed hydrogen beams in background gas. A multi-pixel photon counter (MPPC) is a type of silicon photomultiplier that uses multiple avalanche photodiodes operating in Geiger mode to count photons at low light levels. Using an MPPC, Morris *et al.* [29] found that the light pulse induced by a pulsed 65 keV, 40 mA H^- in the LEBT exhibits a transient peak. The length of this peak corresponds to the SCC time, measured by the ion beam transmission through the RFQ.

DISCUSSION AND CONCLUSIONS

Continuous and pulsed beams often require different diagnostic techniques for the investigation of the SCC process. Diagnostics for pulsed beams are often time-resolved, such that the differences between an uncompensated and a compensated beam can be compared. Diagnostics that require scanning or sweeping, such as wire scanners, many emittance meters or Langmuir probes are useful for continuous beams that will maintain a steady state after the initial transient and are used to determine the ideal gas pressure for the SCC process.

The charge state of the ion beam may also affect the diagnostic technique used if measuring the secondary particles, such as with an RFA. In the case of a negative ion beam, the electrons created through the ionisation reaction could be measured to determine the potential of the beam. However, no electron suppression correction can be applied when measuring electrons with an RFA; a negative bias on the electron suppression grid would act as a retarding field to the low energy electrons repelled by the beam potential. The repelled electrons are also likely to be bound by the solenoid field lines, restricting their movement into an RFA. These magnetic fields also affect the SCC process [23].

Finally, many of the diagnostics detailed in this paper (e.g. beam profile monitors, scintillation viewers, emittance meters) are invasive. The ion beam being measured is not necessarily the same ion beam undergoing the SCC process during typical running conditions.

Weissman [30] reported that measured emittance values of a 20 keV, 5 mA continuous H^+ beam could change by up to 20 % due to secondary electrons emitted from a slit collimator. In experiments to test SCC time, Spädtke [31] inserted a wire grid harp used for beam profile measurements. The secondary electrons produced by this wire grid reduced the SCC time of the pulsed 5 keV, 200-400 µA He^+ beam from 3.5 ms to less than 100 µs.

Simulations using a particle-in-cell (PIC) code, PICLas, of 65 keV, 30 mA H^+ or H^- beams (2.5 cm radius) show changes to the SCC time and degree when a measurement device is placed in the beam path. The simulated ratios of compensating particles to beam particles are shown in Fig. 4. This ratio can be taken as an average measure of the beam potential drop averaged over the simulation domain (0.2 m long cylinder with a 5 cm radius). The residual H_2 gas pressure was set to 1 x 10^{-5} mbar.

The inclusion of a diagnostic device changes the positive z longitudinal boundary condition from a Neumann boundary ($E_z = \nabla\phi \cdot \hat{n} = 0$) without the device to a Dirichlet boundary ($\phi = 0$) with the device inserted, which affects the transport of secondary ions. The device also provides a source of secondary electrons, simulated with two 5 eV electrons emitted per incident ion [32]. These electrons are quickly expelled for an H^- beam but provide an additional source of compensation for an H^+ beam. The use of such invasive techniques therefore has an especially large effect on the SCC process in a positive beam.

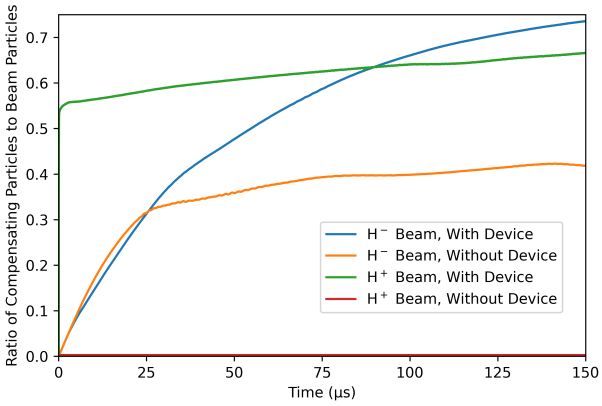

Figure 4: Compensating particle accumulation for the first 150 µs of a 65 keV, 30 mA H^+ and H^- beam in a 0.2 m cylinder simulated domain. The boundary conditions were changed to simulate insertion of an invasive diagnostic.

These results underline the importance of complementing experimental measurements using SCC diagnostics with supporting particle-in-cell simulations to fully understand the SCC process during typical running conditions. It also demonstrates that the use of non-invasive diagnostic techniques alongside spatial dimension or emittance measurements can provide valuable information about the SCC process in a beam.

ACKNOWLEDGEMENTS

This work is supported by the International Science Partnerships Fund (ISPF) grant awarded by UK Research and Innovations and STFC's Ada Lovelace Centre.

REFERENCES

[1] N. Chauvin *et al.*, "Transport of intense ion beams and space charge compensation issues in low energy beam lines", *Rev. Sci. Instrum.*, vol. 83, p. 02B320, 2012. doi:10.1063/1.3678658

[2] M. E. Rudd, "User-friendly model for the energy distribution of electrons from proton or electron collisions", *Nucl. Tracks Radiat. Meas.*, vol. 16, no. 2/3, pp. 213-218, 1989. doi:10.1016/1359-0189(89)90052-6

ISBN: 978-3-95450-262-2 ISSN: 2673-5350 doi: 10.18429/JACoW-IBIC2025-TUDI01

[3] A. P. Letchford *et al.*, "Status of the RAL Front End Test Stand", in *Proc. IPAC'15*, Richmond, VA, USA, May 2015, pp. 3959–3961. doi:10.18429/JACoW-IPAC2015-THPF105

[4] T. Kalvas, "Ion beam intensity and phase space measurement techniques for ion sources", *Rev. Sci. Instrum.*, vol. 93, p. 011501, 2022. doi:10.1063/5.0075110

[5] K. Unser, "A toroidal DC beam current transformer with high resolution", *IEEE Trans. Nucl. Sci.*, vol. NS-28, no. 3, 1981. doi:10.1109/TNS.1981.4331686

[6] T. A. Bykov *et al.*, "Use of a wire scanner for measuring a negative hydrogen ion beam injected in a tandem accelerator with vacuum insulation", *Instrum. Exp. Tech.*, vol. 61, no. 5, pp. 713-718, 2018. doi:10.1134/S0020441218050159

[7] S. X. Peng *et al.*, "Key elements of space charge compensation on a low energy high intensity beam injector", *Rev. Sci. Instrum.*, vol. 84, p. 033304, 2013. doi:10.1063/1.4794966

[8] H. von Jagwitz-Biegnitz *et al.*, "2D Wire Grid Integrated with Faraday Cup for Low Energy H- Beam Analysis at Siemens Novel Electrostatic Accelerator", in *Proc. IBIC'13*, Oxford, UK, Sep. 2013, paper TUPF06, pp. 507–510.

[9] P. Y. Beauvais, "Space Charge Neutralization Experiment with a Low Energy Proton Beam", in *Proc. LINAC'96*, Geneva, Switzerland, Aug. 1996, paper MOP57, pp. 202–204.

[10] V. Toivanen, "The effects of beam line pressure on the beam quality of an electron cyclotron resonance ion source", *Nucl. Instrum. Methods Phys. Res. B.*, vol. 268, no. 9, 2010, pp.1508-1516. doi:10.1016/j.nimb.2010.01.016

[11] A. Misra *et al.*, "Studies on space charge neutralization and emittance measurement of beam from microwave ion source", *Rev. Sci. Instrum.*, vol. 86, p. 113301, 2015. doi:10.1063/1.4934868

[12] Y. K. Batygin, "Dynamics of intense particle beam in axial-symmetric magnetic field", *Nucl. Instrum. Methods Phys. Res. A.*, vol. 7726, pp. 93-102, 2015. doi:10.1016/j.nima.2014.10.034

[13] A. L. Zhang *et al.*, "Study on space charge compensation in negative hydrogen ion beam", *Rev. Sci. Instrum.*, vol. 87, p. 02B915, 2016. doi:10.1063/1.4932557

[14] C. A. Valerio-Lizarraga, *et al.*, "Space charge compensation in the Linac4 low energy beam transport line with negative hydrogen ions", *Rev. Sci. Instrum.*, vol. 85, p. 02A505, 2014. doi:10.1063/1.4847196

[15] C. A. Valerio-Lizarraga, I. Leon-Maonzon and R. Scrivens, "Negative ion beam space charge compensation by residual gas", *Phys. Rev. ST Accel. Beams*, vol. 18, p. 080101, 2015. doi:10.1103/PhysRevSTAB.18.080101

[16] P. W. Allison, J. D. Sherman, and D. B. Holtkamp, "An Emittance Scanner for Intense Low-Energy Ion Beams", *IEEE Trans. Nucl. Sci.*, vol. 30, no. 4, pp. 2204-2206, 1983. doi:10.1109/TNS.1983.4332762

[17] M. Cavenago, M. Comunian, E. Fagotti, T. Kulevoy, S. Petrenko, and M. Poggi, "High Current Ion Sources, Beam Diagnostics and Emittance Measurement", in *Proc. HIAT'09*, Venice, Italy, Jun. 2009, paper E–06, pp. 341–345.

[18] R. Gobin *et al.*, "Improvement of beam emittance of the CEA high intensity proton source SILHI", *Rev. Sci. Instrum.*, vol. 70, no. 6, 1999. doi:10.1063/1.1149823

[19] R. Doelling, P. Grobeta, H. Klein, J. Pozimski, and K. Reidelbach, "Plasma Potential and Temperature Measurements of a Thin Plasma by use of Langmuir-Probes", in *Proc. EPAC'94*, London, UK, Jun.-Jul. 1994, pp. 1755–1758.

[20] A. J. Holmes, "Theoretical and experimental study of space charge in intense ion beams", *Phys. Rev. A*, vol. 16, no. 1, p. 389, 1979. doi:10.1103/PhysRevA.19.389

[21] P. Kreisler, H. Baumann, K. Bethge, "Measurements of space charge compensation of ion beams", *Vacuum*, vol. 34, no. 1-2, pp. 215-216, 1984. doi:10.1016/0042-207X(84)90130-1

[22] K. Reidelbach, R. Doelling, P. Grobeta, A. Jacob, H. Klein, and J. Pozimski, "Investigations of Space charge Compensation of Pulsed Ion Beams", in *Proc. EPAC'94*, London, UK, Jun.-Jul. 1994, pp. 1758–1761.

[23] B. John *et al.*, "Effect of magnetic field on space charge compensation in negative hydrogen ion beams: a computational study", *J. Instrum.*, vol. 20, p. C05024, 2025. doi:10.1088/1748-0221/20/05/C05024

[24] Z. Shen *et al.*, "Space charge compensation study of high intensity ion beams", *J. Phys: Conf. Ser.*, vol. 2244, p. 012090, 2022. doi:10.1088/1742-6596/2244/1/012090

[25] D. Winklehner *et al.*, "Space-charge compensation measurements in electron cyclotron resonance ion source low energy beam transport lines with a retarding field analyzer", *Rev. Sci. Instrum.*, vol. 85, p. 02A739, 2014. doi:10.1063/1.4854315

[26] J. Sherman, P. Allison, and E. Pitcher, "H Beam Neutralization Measurements with a Gridded-Energy Analyser, a Non-interceptive Beam Diagnostic", in *Proc. LINAC'88*, Williamsburg, VA, USA, Oct. 1988, paper MO3–44, pp. 155–157.

[27] R. Ferdinand, "Space-Charge Neutralization Measurement of a 75-keV, 130-mA Hydrogen-Ion Beam", in *Proc. PAC'97*, Vancouver, Canada, May 1997, paper 6W010, pp. 2723–2725.

[28] C. Ullmann *et al.*, "Investigation of ion beam space charge compensation with a 4-grid analyzer", *Rev. Sci. Instrum.*, vol. 87, p. 02B938, 2016. doi:10.1063/1.4939782

[29] D. Morris *et al.*, "Microwave driven space-charge compensation with optical diagnostics and feedback", in *Proc. IPAC'23*, Venice, Italy, May 2023, pp. 2767–2769. doi:10.18429/JACoW-IPAC2023-WEPA049

[30] L. Weissman, "Effect of secondary electrons suppression on emittance measurement of an intense, low-energy beam", *Rev. Sci. Instrum.*, vol. 85, p. 02A710, 2014. doi:10.1063/1.4827115

[31] P. Spädtke, "The role of space charge compensation for ion beam extraction and ion beam transport", *Rev. Sci. Instrum.*, vol. 85, p. 02A744, 2014. doi:10.1063/1.4862661

[32] A. K. Fazlul Haque *et al.*, "Proton-induced secondary electron emission from elemental solids over the energy domain 1 keV-1000 MeV", *Results Phys.*, vol. 15, p. 102519, 2019. doi:10.1016/j.rinp.2019.102519